La^{−} binding energies by analysis of its photodetachment spectra

Lin Pan and Donald R. Beck

Phys. Rev. A **93**, 062501 — Published 1 June 2016

DOI: 10.1103/PhysRevA.93.062501

Study of La^- binding energies by analysis of its photodetachment spectrum

Lin Pan*
Science and Mathematics Department, Cedarville University, Cedarville, Ohio 45431, USA

Donald R. Beck
Physics Department, Michigan Technological University, Houghton, Michigan 49931, USA
(Dated: January 11, 2016)

This study reinterprets an earlier experimental photoelectron kinetic energy spectrum of the negative ion of lanthanum [A. M. Covington, D. Calabrese, J. S. Thompson and T. J. Kvale, J. Phys. B **31**, L855 (1998)] by carrying out relativistic configuration interaction (RCI) photodetachment calculations. The results confirm the earlier RCI calculation for the electron affinity of lanthanum (0.545 eV) [S. M. O'Malley and D. R. Beck, Phys. Rev. A. **79**, 012511 (2009)] and revise it to a slightly larger value of 0.550 eV, thus modifying the experimental interpretation of 0.47 ± 0.02 eV. The calculation also yields the binding energies of the other thirteen bound states of La^-. Good agreement has been found when these energies are compared to the results of a recent experimental study on La^- [C. W. Walter, N. D. Gibson, D. J. Matyas, C. T. Crocker, K. A. Dungan, B. R. Matola, and J. Rohlén, Phys. Rev. Lett. **113**, 063001 (2014)]. Finally, our analysis confirms the transition energy for the potential laser cooling transition of $^3F_2^e \rightarrow {}^3D_1^o$ in La^-.

PACS numbers: 32.10.Hq, 31.15.am, 32.80.Gc

I. INTRODUCTION

Laser cooling of atomic anions has been proposed as an effective way of preparing ultracold antiprotons through sympathetic cooling [1]. To be laser cooled, the atomic anion must have bound states of opposite parities that are connected by, ideally, an electric-dipole ($E1$) transition. Few anions possess this property and so far, only three atomic negative ions, Ce^- [2], Os^- [1, 3, 4] and La^- [5, 6] have been identified as possible candidates for laser cooling of negative ions. Among them, La^- is deemed the most promising [6, 7] due to the large strength of the proposed laser-cooling $E1$ transition, the short lifetime of the excited state and the large branching ratio to the initial state [8], all of which are essential to efficient laser cooling.

However, the electronic properties of La^- have not been fully studied. As evidence, while there have been various theoretical [9–15] and experimental [6, 7, 16, 17] studies of the bound state structure of La^-, the value of the electron affinity (EA) of La and the binding energies of most La^- states are still unsettled.

In 1998, Covington *et al.* [16] measured the electron affinity for lanthanum using the laser photoelectron energy spectroscopy (LPES) technique. Their analysis of the photoelectron kinetic energy spectrum indicated the ground state of La^- to be bound by 0.47 ± 0.02 eV, and that La^- has at least one excited state which is bound by 0.17 ± 0.02 eV. Today, after almost two decades, this remains the only measurement of EA for lanthanum.

In 2009, equipped with an improved technique in doing relativistic configuration interaction (RCI) calculations, O'Malley and Beck recalculated the binding energies of lanthanum during a survey of all lanthanide and actinide anions [15]. Their investigation revealed the La^- ground state configuration should be $5d^2\ 6s^2$, instead of $5d\ 6s^2\ 6p$ as had been held earlier [12–14]. Seven even-parity bound states ($5d^2\ 6s^2$) and eight odd-parity bound states ($5d\ 6s^2\ 6p$) were identified, with the EA of the ground state ($^3F_2^e$) computed to be 0.545 eV. Comparing to the experimental result of 0.47 ± 0.02 eV [16], this computed EA value is about 0.07 eV larger.

Recently, Walter *et al.* [6] applied to La^- tunable infrared laser photodetachment threshold spectroscopy (LPTS) in the photon energy range of 0.295 - 0.585 eV. All electric dipole bound-bound transitions in the energy range were identified and measured, including that of the potential laser cooling transition of $^3F_2^e \rightarrow {}^3D_1^o$. The observed transitions were used to determine the relative energies of the $^3F_{3,4}^e$, $^3F_{2,3,4}^o$, $^3D_{2,3,4}^o$ excited states to the ground state of $^3F_2^e$. Besides, the binding energy of the $^1D_2^o$ state was measured to be 0.3356(8) eV. These results indicate the RCI calculations [15] have positioned the odd-parity states ($5d\ 6s^2\ 6p$) 0.062 - 0.098 eV too close to the ground state and the $5d^2\ 6s^2\ ^3F_3$, $^3F_4$ even-parity states 0.017 eV, 0.038 eV respectively too close to the ground state. The EA of lanthanum was not the focus and therefore not measured in their study.

Most recently, two high-resolution spectroscopy studies have been conducted for two individual $E1$ transitions in La^-. One was by Jordan and co-workers [7], who measured the transition energy of the potential laser cooling transition of $^3F_2^e \rightarrow {}^3D_1^o$. Their result of 399.4757(4) meV (96.59280(10) THz) is in excellent agreement with the earlier measurement of 399.42(3) meV by Walter *et al.* [6]. The other measurement [17] was by Kellerbauer *et al.* for the transition of $^3F_2^e \rightarrow {}^3F_2^o$. Their result of 343.6868(15) meV was again

*Electronic address: lpan@cedarville.edu

in excellent agreement with the earlier measurement of 343.69(3) meV by [6].

The work presented here aims at determining the EA and binding energies (BEs) of lanthanum. As a check of our calculations, we will confirm the potential laser-cooling transition energy measured by Walter *et al.* [6] and Jordan *et al.* [7], as well as other transition energies determined in [6] and by Kellerbauer *et al.*[17]. Our approach is to identify the dominant features in the electron kinetic energy spectrum in [16] through a photodetachment calculation. Earlier, this approach has been used by O'Malley and Beck [18] to determine the EA of Ce^- and their reinterpreted value of 0.660 eV was in good agreement with a later LPTS analysis of 0.628 ± 0.010 eV [2]. For La^-, the same approach has been suggested by O'Malley and Beck [15] when trying to explain the discrepancy between their calculated EA of 0.545 eV and the LPES value of 0.47 ± 0.02 eV [16].

II. COMPUTATIONAL METHODOLOGY

The methodology employed in this study is relativistic configuration interaction (RCI). Details of the RCI formalism can be found elsewhere [19]. Below, only a brief explanation of RCI is summarized.

RCI calculations begin with generating one-electron basis sets for orbitals occupied in the reference configurations. This is realized using the Multi-Configuration Dirac-Fock (MCDF) program of Desclaux [20]. The next step is to construct many-electron wave functions which are eigenvectors of J^2, J_z, and parity and are expressed as linear combinations of antisymmetrized determinants of the one-electron basis functions. Next, correlation effects are introduced into the wave function by adding configurations which represent single or double replacements of valence electrons in the reference configuration(s). The replacing orbitals that are not occupied in the reference configuration(s) are represented by virtual orbitals in the form of the relativistic screened hydrogenic function (SHF). Each SHF has only one adjustable parameter, the effective charge (Z^*), which is estimated and then optimized during the energy variational process of RCI. Typically, two sets of virtual orbitals are required for a sufficient capture of correlation effects. Orbitals of the same symmetry (l, j), either occupied or virtual, are made orthogonal to each other.

The photodetachment process can be described as: $A^- + h\nu \rightarrow A + \epsilon$. where A^- stands for the initial bound state of the anion, $h\nu$ is the energy of the incident photon, $A + \epsilon$ is the final continuum state consisting of the neutral state A and the ejected photoelectron ϵ.

The La^- even-parity states, $5d^2\ 6s^2$, can detach into either the $5d\ 6s^2$ channels or the $5d^2\ 6s$ channels. The potential channels are restricted by the photon energy. For example, while the configuration $5d^3\ 6s$ has an almost constant mixing of 10% in the $^3P_{0,1,2}$ excited states, their presence leads to trivial 6s detachment into the $5d^3$ channels. Analysis reveals the $5d^3$ subgroup in La^- $5d^3\ 6s$ is dominantly ^2P, but the energetically-accessible $5d^3$ thresholds are dominated by either ^4F, ^4P or ^2G respectively. As for the *LS*-favorable $5d^3\ ^2P$ thresholds, they lie too high in the spectrum for the given photon energy. The La^- odd-parity states of $5d\ 6s^2\ 6p$ present a richer detachment scheme. In the wave function for La^- $5d\ 6s^2\ 6p$, there is always a non-trivial mixing of $5d^2\ 6s\ 6p$, ranging from 17% to 27%. This suggests that the odd states can detach into channels of $5d\ 6s^2$, $6s^2\ 6p$, $5d\ 6s\ 6p$, as well as channels of $5d^2\ 6s$, $5d^2\ 6p$. The mixing of $5d^3\ 6p$, however, is always small ($< 4\%$), indicating its 6p detachments into the $5d^3$ channels are small, as our calculations have shown.

The wave functions for the bound states of La^- are generated using single and double valence RCI. The core is kept closed and so no core-valence or core-core correlation is included. While this may be inadequate for energy calculations, it is appropriate for photodetachment cross section studies for two reasons. First, the energy values have been computed by RCI [15] and so we can simply quote the results and then adjust their values. Secondly, having the correct mixing of configurations is crucial in cross section calculations and valence RCI runs are sufficient for this need.

The wave function for the final continuum-state is generated using a frozen-core approximation, where the wave function of a free electron is attached to that of a neutral state [21]. The one-electron wave function of the free electron is assumed to have the same angular form as that of a bound electron of the same symmetry. Its radial function is numerically generated in a frozen-core Dirac-Fock potential, using a modified version [21] of the relativistic continuum wave solver of Perger *et al.* [22, 23]. The radial function of the free electron is made orthogonal to each radial function of the same symmetry (l, j) in the neutral core.

Like La^-, the wave functions for the La thresholds are generated using valence RCI. Given the incident photon's energy in the LPES experiment [16] was 2.410 eV (514.5 nm), and the carried-away energy by the ejected photoelectrons was greater than 0.15 eV, the neutral thresholds that can be reached during the photodetachment must lie within at most 2.26 eV above the ground state, La $5d\ 6s^2$ $^2D_{3/2}$. Since the energy values of La excited states are established and available [24], we are only concerned with the proper mixing of the eigenvectors, which is indicated by the Landé g values in the RCI wave functions. This is where our deviation from a pure *ab initio* calculation comes into play. To improve the Landé g values to within 0.01 of the experimental values, we have used "shifts", where the main diagonal energy matrix element of a reference basis vector is shifted downward. As an example, for La odd-parity ($5d\ 6s\ 6p$) $J = 1/2$ states, while the experimental g values are 0.357 for its ground state and 0.313 for the first excited state, our RCI g values were 0.646 and 0.031 respectively. Analysis of the RCI wave function revealed that the problem was due to the two

dominant configurations, $6s^2$ 6p and 5d 6s 6p, not mixing properly in the RCI wave function. By shifting down two LS basis vectors of 5d 6s 6p, $(^3D)^4D$ and $(^3D)^2P$, by about 0.5 eV each, the RCI g values are improved to 0.356 (ground state) and 0.316 (first excited state), in excellent agreement with the experimental values.

It is interesting that throughout this process of improving the Landé g values, the sum of the g values of these two $J = 1/2$ states remains almost constant. While the sum of experimental values is 0.677, the RCI sums are 0.670 before applying shifts and 0.672 after applying shifts. This 'conservation rule' has been observed by Beck and Abdalmoneam [25], stating that the sum of the g-values of nearby levels of the same J and parity is nearly constant.

The cross section is calculated using [26]:

$$\sigma = 4\pi^2 \alpha\, a_0^2 \frac{df}{dE} = 8.067 \times 10^{-18} \frac{df}{dE}\ (\mathrm{cm}^2), \quad (1)$$

where α is the fine-structure constant, a_0 is the Bohr radius, and $\frac{df}{dE}$ is the differential oscillator strength for the electric-dipole ($E1$) transition from the La^- initial bound state to the final continuum state. The formalism for RCI cross section calculations is summarized in our recent work [27]. Briefly, the $\frac{df}{dE}$ term is evaluated using a modified version [28] of our code for bound-bound transitions [19, 29]. We use the Babushkin gauge (the relativistic analog of length gauge) of the $E1$ operator. This gauge has shown to be stable over small changes in basis set size. The rigor of this modified version has been tested in a similar calculation that revised the experimental interpretation for Ce^- [18] and in a more recent calculation on Ce^- [2] which refined its EA and BEs.

Given the anion state, its calculated cross section into a neutral threshold is a summation over cross sections of all allowed relativistic channels. To illustrate, for 5d $6s^2$ 6p $^1D^o_2 \rightarrow$ 5d $6s^2$ $^2D_{3/2}$ + ϵs/ϵd, the cross section is the sum over eight relativistic channels: two $\epsilon s_{1/2}$ channels with total $J = 1$, 2, three $\epsilon d_{3/2}$ channels and three $\epsilon d_{5/2}$ channels, each with total $J = 1$, 2, 3.

III. RESULTS AND DISCUSSION

Our strategy in interpreting the photoelectron kinetic energy spectrum of Covington *et al.* (shown in Fig. 2) consists of four steps. First, for each La^- bound state predicted by earlier RCI calculation [15], its individual photodetachment cross sections into all energetically accessible neutral states are computed, with the energy of the incident photon being fixed at 2.41 eV, the same value as in the experiment. To simulate the number of electrons ejected in the experiment, the population distribution of the La^- states in the ion beam is taken into account. While there is no direct way to obtain the real distribution, this is simulated by a multiplicative Boltzmann factor applied to the calculated cross section, assuming a thermal energy distribution. The effective temperature of kT was chosen to be 0.17 eV, corresponding to an ion beam temperature of about 2000 K. It has been shown the choice of kT's value affects very little the shape of the simulated spectrum [18], but still, at the final stage of the simulation, we have tried a different effective temperature of 0.12 eV ($\sim$ 1400 K) and included the result in Fig. 5. In addition to the Boltzmann factor, the multiplicity value $(2J + 1)$ for each initial La^- state is also included to simulate population distribution.

For the second step, the population-weighted cross sections from all La^- bound states are convoluted and added up, yielding the simulated electron kinetic energy spectrum. Next, the features in the simulation are moved so that they line up with the features in the experimental spectrum. This is accomplished by adjusting the BE of the corresponding individual La^- bound state. Finally, we recalculate the cross sections from those bound states whose BEs have been adjusted dramatically. By experience, we do not expect cross sections to change significantly with a small change in BE. Our calculations in this study have again verified this.

The earlier RCI calculation [15] has predicted seven bound even-parity states and eight bound odd-parity states. We calculated photodetachment cross sections from each of these states and convoluted them into simulated electron counts, except for the La^- $^3P^o_0$ state. This was the least bound state (by 10 meV) and so we don't expect it to have a significant population in the ion beam used in the experiment. Besides, calculations carried out during this study seem to indicate that this $^3P^o_0$ state is unbound. With the $^3P^o_0$ state excluded, the number of bound states included in the simulation becomes fourteen.

To facilitate discussions, we have plotted simulated electron counts from each of the fourteen bound states in Fig. 1. They correspond to our final simulated spectrum using the EA and BEs determined in this study. Each "bar" represents the population-weighted cross section to a specific non-relativistic neutral threshold. Only thresholds with a weighted cross section of 1.5% or larger of the strongest detachment (La^- $^3F^e_2$ into La 5d^2 6s $^4F^e_{3/2}$) are plotted in Fig. 1. The weaker thresholds are not plotted as they will be too small to be noticeable for the scale employed. "Bar"s produced by the same initial La^- state are, as expected, separated at distances equal to the energy separations between the corresponding neutral thresholds whose energy values have been established [24].

According to [16], only the part of the spectrum beyond 0.15 eV is due to photodetachment of La^-. Accordingly, the kinetic energy in the simulation starts at 0.155 eV and ends at 2.4 eV. Looking at the experimental spectrum (included in Fig. 2) while referring to Fig. 1, it can be observed, from left to right, that peak 6 is completely due to the odd-parity states of 5d $6s^2$ 6p, mainly $^1D^o_2$; that peaks 5 and 4 are produced by the even-parity states of 5d^2 $6s^2$, among which $^3F^e_{2,3,4}$ and $^1D^e_2$ dominate; also that the $^3F^e_{2,3,4}$ states contribute dominantly to peak

3, in addition to the less significant $^1D^o_2$ state. Finally, peaks 2 and 1 are dominated by the odd-parity 5d 6s^2 6p states, with a decent contribution from the 5d^2 6s^2 $^1D^e_2$ state to peak 2.

The simulated spectrum using the earlier RCI EA and BEs [15] are shown in Fig. 2. In making the simulation plot, each photodetachment cross section is represented, at the corresponding electron kinetic energy, by a Gaussian with a full-width-at-half-maximum (FWHM) of 0.040 eV, chosen to match the overall envelope of the experimental plot. All the Gaussians are then summed up to obtain the simulated spectrum.

In Fig. 2, six prominent features are easily identified which have a one-to-one correspondence with the six peaks in the experimental spectrum. Roughly speaking, peaks 3, 4 and 5 in the simulated spectrum line up well with the corresponding peaks in the experimental spectrum, indicating that the RCI BEs for the contributing states to these peaks, i.e., the La$^-$ 5d^2 6s^2 ^{3}F$^e_{2,3,4}$ states, are close to the true values. It can be observed that peak 3 and peak 5 are narrower than the corresponding ones in the experimental plot, thus indicating that the relative energies of the ^{3}F$^e_{2,3,4}$ states need adjustment. On the other hand, both peak 1 and peak 2 in the simulated plot show a large shift toward the lower kinetic energy end as compared to the measured spectrum. This suggests that the earlier RCI BEs for the component states of 5d 6s^2 6p were overestimated, resulting in the ejected photoelectrons to have lower kinetic energy in the simulation.

Our next step is to adjust the RCI BEs. As a starting point, we made use of measurements by Walter *et al.* [6] which are relative energies above the La$^-$ $^3F^e_2$ ground state. Namely they are the two even-parity states ($^3F^e_{3,4}$) and all the odd-parity states. Since EA was not measured in [6], we used the RCI EA value and inferred the BEs of these excited states based on their measured relative energies. For BEs of the $^1D^e_2$ and $^3P^e_{0,1,2}$ states, we kept their RCI values as they were not measured in [6]. Meanwhile at this stage, we have improved our wave function for the neutral thresholds by improving their Landé g values. With these, the cross sections were recalculated. It turns out, however, a small improvement in the g value usually does not make any significant change to the cross section. The simulated spectrum is shown in Fig. 3.

As can be seen, the simulation at this stage shows a much better agreement with the experiment. Among all the odd-parity states, the most significant change has occurred to the ^{1}D$^o_2$ $\rightarrow$ 5d 6s^2 ^{2}D$^e_{3/2}$ + ϵs/ϵd channel which experiences a large decrease in its contribution. As indicated in Fig. 1, this is a strong channel by itself. However, according to [6], the ^{1}D$^o_2$ state is about 0.1 eV less bound with a measured BE of 0.3356(8) eV. While a change of 0.1 eV in photoelectron energy usually does not affect cross sections dramatically, it causes the simulated population of the ^{1}D$^o_2$ state to decrease by almost a factor of 2 (at effective temperature of 0.17 eV). As a result, the simulated peak 2 in Fig. 3 is much smaller and is at a higher kinetic energy than that in Fig. 2, thus bringing better agreement with peak 2 in the experimental plot.

Another change is in the shape and width of peak 3 and peak 5. Now that the inferred BE for the $^3F^e_4$ state is almost 40 meV smaller than the RCI value, the "bar"s due to the detachment of $^3F^e_4$ are moved toward the higher kinetic energy end, away from the "bar"s due to the detachment of $^3F^e_2$. The "bar"s due to the detachment of $^3F^e_3$ have been moved in the same direction, only by a smaller amount due to a smaller decrease of 17 meV in its inferred BE. As a result, peak 5 and peak 3 in the simulated plot both acquire an obvious shoulder and become wider.

Comparing to the experimental plot, the largest difference is now in peaks 6 and 5. They remain small in the simulation, resulting in peak 4 being the largest peak instead of peak 5. This issue will be addressed later in the manuscript.

A closer examination shows the simulated peaks 1 to 5 are shifted either to the left or to the right of their counterparts in the experimental plot, by varying amounts. Next, the amount of adjustment required for each BE (inferred or the original RCI values) was determined by trial and error. Finally, as a more stringent test [30] of our adjusted EA and BEs, the updated simulated spectrum is compared to the inset in the experimental spectrum (in Fig. 1 of [16], reproduced here in Fig. 4). The inset graph is a separate electron kinetic energy spectrum over the higher energy region that includes peaks 1 to 3. It was measured at twice the accumulation time per data point, with the same frequency but more powerful laser. The simulated inset spectrum (Fig. 4) was plotted using a smaller FWHM of 0.020 eV to reveal more of the individual features that contribute to peaks 1 to 3. The experimental inset graph shows peak 2 contains at least two bumps, with a broader one on the left and one or two narrower ones on the right. Our calculation shows the broader one is due to detachment of ^{3}F$^o_2$ into La 5d 6s^2 ^{2}D$_{5/2}$ (see Fig. 1), by which the BE for ^{3}F$^o_2$ is revised and determined in this work. The corresponding bump in our simulation was too weak, however, resulting in it being "absorbed" by the larger and narrower one on its right in the final simulated spectrum in Fig. 5, where a larger FWHM of 0.040 eV was used. The simulation using the revised EA and BEs in Fig. 5 looks very similar to the one in Fig. 3 due to small changes to EA and BEs. The largest improvement occurs to the region including peaks 1 to 3.

The revised EA and BEs are listed in Table 1. For the even-parity La$^-$ states, it turns out the RCI EA and RCI BE for the ^{3}F$^e_3$ state were accurate, changed only by 5 meV, 7 meV respectively in the revised values. As for the ^{3}F$^e_4$ state, we agree with Walter *et al.* [6] that it should be less bound by about 30 meV. Our revised relative energies (shown in Table 1) of the ^{3}F$^e_3$, ^{3}F$^e_4$ states are in good agreement with results in [6], with a difference of only 5 meV in each state and in the same direction. No measurement is available for the ^{1}D$^e_2$ and ^{3}P$^e_{0,1,2}$ states.

The $^1D^e_2$ state plays a big role in forming peak 2 and we found its earlier RCI BE was accurate and only needs to be increased by 10 meV. The $^3P^e_{0,1,2}$ states contribute to the features in the valley between peaks 4 and 5. Due to the smallness of these features, the not so high resolution and a concern for the energy calibration in the lower-energy region of the experimental spectrum, their BEs are the least accurately determined in this work.

For the $^3F^o_{2,3,4}$, $^3D^o_{1,2,3}$ odd-parity states, we agree well with [6] in relative energy values. As shown in Table 1, the differences are between -10 meV to 8 meV. Our simulations have thus confirmed Walter *et al.*'s results that the earlier RCI calculations have positioned these $^3F^o$, $^3D^o$ states too low relative to the $^3F^e_2$ ground state. The only other odd state is $^1D^o_2$. We found it needs to be 20 meV (the uncertainty stated in [16]) less bound than that measured in [6].

Another way to compare to the experiment is through the transition energy values. For the $E1$ transitions measured by Walter *et al.* in [6], the agreement in the transition energies is good, with the difference varying between -8 meV and 15 meV (our work - [6]). For the $^3F^e_2 \rightarrow {}^3F^o_2$ transition and the potential laser cooling transition of $^3F^e_2 \rightarrow {}^3D^o_1$, the comparison to [6] and other recent experimental results can be found in Table 1, where the tabulated relative energy is just the transition energy in these two cases. As shown, the differences are about 5 meV and -5 meV respectively.

Bearing in mind one goal is to determine the EA of La, we have identified from our simulation the small spike (in Fig. 4, at about 1.7-1.8 eV) in the valley between peak 3 and peak 4 to be produced by the photodetachment of La^- ground state, $5d^2\ 6s^2\ {}^3F^e_2$, into the first excited state of La, $5d\ 6s^2\ {}^2D_{5/2}$ (at 0.1306 eV [24]). This detachment is almost ten times weaker than the detachment into the neutral ground state $5d\ 6s^2\ {}^2D_{3/2}$, which is embedded in peak 3. Formerly, both thresholds were thought to be inside peak 3, leading to an underestimated EA of 0.47 ± 0.02 eV [16]. (It should be mentioned that no knowledge of the LS or JJ compositions of the La^- bound states was available at the time the spectrum was interpreted. Later, RCI calculations [15] revealed the JJ compositions of La^- $5d^2\ 6s^2$ which shows the ground state ($^3F^e_2$) can only make a strong detachment into the La $5d\ 6s^2\ {}^2D_{3/2}$ threshold but not the ${}^2D_{5/2}$ threshold, as has been confirmed by our calculations in this work). In the inset of the experimental spectrum, the spike appears to be at between 1.71 eV and 1.76 eV. Given the photon's energy being 2.410 eV and the threshold being at 0.1306 eV, the EA can be computed and found to be between 0.52 eV and 0.57 eV. Our revised RCI EA of 0.550 eV falls into this range.

Although peaks 5 and 6 do not interfere with our goal of determining the EA and even the BE of La^- excited states, we want to give some insight into the discrepancy. Through the simulation, we have found the dominant contributor to peak 6 and peak 2 to be the same, i.e., $5d\ 6s^2\ 6p\ {}^1D^o_2$. As a result, the energy separation between the centroids of these two peaks should be approximately the energy separation between the corresponding neutral thresholds. Our calculations show (see Fig. 1) they are the La ground state $5d\ 6s^2\ {}^2D_{3/2}$ (for peak 2) and 5d 6s 6p ${}^4F_{5/2}$ state (for peak 6), whose energy separation is about 1.690 eV [24]. However, in the experimental spectrum, the separation is about 1.76 eV. It can be observed from Fig. 5 that while the shapes of the simulated and the experimental spectra are very similar, there is an increasingly large shift between the two spectra as one moves toward the lower energy end. We therefore wonder the energy calibration and the collection efficiency in the experiment to play a big role in the discrepancy, especially in the lower energy region below 1.5 eV. Secondly, the relative intensity of peaks 5 and 6 are too small comparing to the other peaks. Two reasons might contribute to this. The first is the omission of polarization potential when generating wave functions for the final continuum states. It is known that polarization of the neutral core has an impact on near-threshold photodetachment behaviors [31]. Since peak 6 is due to detachment into the high-lying 5d 6s 6p channels, leaving the photoelectron with low energy of several tenths of electron volts, the polarization effect could be significant to the corresponding photodetachment cross sections. The other reason might be due to the angular-dependence of the differential cross section. Since the polarization angle of the laser beam is not provided in [16], we have assumed the angle to be the magic angle which "removes" the angular dependence of the differential cross section. If the polarization angle is not the magic angle, however, one will also need to take into account the asymmetry parameter (β) of the photoelectron. Both peaks 5 and 6 are due to a $6s \rightarrow \epsilon p$ detachment, where β has the largest possible value of 2. Combined with a favorable polarization angle, a larger β will contribute to a larger differential cross section and therefore larger relative intensity. Finally, the experimental spectrum seems to have an exponential background which lifts up peaks 5 and 6. No such background has been introduced in our simulation. Despite of the ambiguity, it is the higher energy part of the spectrum, not the lower energy region, that is essential to determining the EA and those larger BEs. Our final simulated spectrum seems to indicate the higher energy region was reliably measured in [16].

IV. CONCLUSIONS

In summary, our study of La^- combining previous laser photoelectron energy spectroscopy (LPES) results of Covington *et al.* [16] and calculations of the cross sections has revised the electron affinity (EA) of Lanthanum to be 0.550 eV, thus confirming the earlier RCI EA of 0.545 eV by O'Malley and Beck [15] was accurate and that the experimental interpretation of 0.47 ± 0.02 eV by Covington *et al.* [16] was erroneous. Our work has also revised the RCI predictions for the BEs of

the other 13 bound states of La^-. Excitation energies of these bound states and the (allowed $E1$) transition energies among them derived from our refined EA and BEs are compared to the recent experimental results [6, 7, 17]. Whenever the comparison is applicable, the agreement is good with differences being at most 15 meV. Our analysis of the LPES energy spectrum has also confirmed the transition energy for the potential laser-cooling transition $^3F_2^e \rightarrow {}^3D_1^o$ measured in [6, 7]. Four even-parity states that were not related to any E1 transition in [6] have been revised with new BEs.

It needs to be mentioned that our refined values depend on the quality of the LPES energy spectrum [16]. Given the uncertainty of 20 meV in the experimental work and the ambiguity in matching up some small features in our simulation, it will not be surprising that the refined EA or BEs are uncertain by 20 meV. To further test our results, a tunable laser photodetachment threshold spectroscopy study will be very desirable.

Acknowledgments

This work is based in part upon work supported by the National Science Foundation under Grant No. PHY-0968205. The authors thank Drs. C. W. Walter and N. D. Gibson for their many insightful discussions. Lin Pan especially thanks Dr. C. W. Walter for his many valuable suggestions during the revision of the manuscript.

[1] A. Kellerbauer and J. Walz, New J. Phys. **8**, 45 (2006).
[2] C. W. Walter, N. D. Gibson, Y. -G. Li, D. J. Matyas, R. M. Alton, S. E. Lou, R. L. Field III, D. Hanstorp, L. Pan and D. R. Beck, Phys. Rev. A **84**, 032514 (2011).
[3] U. Warring, M. Amoretti, C. Canali, A. Fischer, R. Heyne, J. O. Meier, Ch. Morhard and A. Kellerbauer, Phys. Rev. Lett. **102**, 043001 (2009).
[4] A. Fischer, C. Canali, U. Warring and A. Kellerbauer, Phys. Rev. Lett. **104**, 073004 (2010).
[5] L. Pan and D. R. Beck, Phys. Rev. A **82**, 014501 (2010).
[6] C. W. Walter, N. D. Gibson, D. J. Matyas, C. T. Crocker, K. A. Dungan, B. R. Matola, and J. Rohlén, Phys. Rev. Lett. **113**, 063001 (2014).
[7] E. Jordan, G. Cerchiari, S. Fritzsche, and A. Kellerbauer, Phys. Rev. Lett. **115**, 113001 (2015).
[8] S. M. O'Malley and D. R. Beck, Phys. Rev. A. **81**, 032503 (2010).
[9] R. J. Zollweg, J. Chem. Phys. **50**, 4251 (1969).
[10] B. M. Angelov, Chem. Phys. Lett. **43**, 368 (1976).
[11] S. G. Bratsch, Chem. Phys. Lett. **98**, 113 (1983).
[12] S. H. Vosko, J. B. Lagowski, I. L. Mayer, and J. A. Chevary, Phys. Rev. A. **43**, 6389 (1991).
[13] E. Eliav, S. Shmulyian, U. Kaldor, and Y. Ishikawa, J. Chem. Phys. **109**, 3954 (1998).
[14] S. M. O'Malley and D. R. Beck, Phys. Rev. A. **60**, 2558 (1999).
[15] S. M. O'Malley and D. R. Beck, Phys. Rev. A. **79**, 012511 (2009).
[16] A. M. Covington, D. Calabrese, J. S. Thompson, and T. J. Kvale, J. Phys. B **31**, L855 (1998).
[17] A. Kellerbauer, G. Cerchiari, E. Jordan, and C. W. Walter, Phys. Scrip. **90**, 054014 (2015).
[18] S. M. O'Malley and D. R. Beck, Phys. Rev. A **74**, 042509 (2006).
[19] D. R. Beck, Phys. Scr. **71**, 447 (2005).
[20] J. P. Desclaux, Comp. Phys. Commun. **9**, 31 (1975).
[21] S. M. O'Malley and D. R. Beck, Phys. Rev. A **77**, 012505 (2008).
[22] W. F. Perger, Z. Halabuka and D. Trautmann, Comput. Phys. Commun. **76**, 250 (1993).
[23] M. G. Tews and W. F. Perger, Comput. Phys. Commun. **141**, 205 (2001).
[24] Yu. Ralchenko, A. E. Kramida, J. Reader, E. B. Saloman, J. E. Sansonetti, J. J. Curry, D. E. Kelleher, J. R. Fuhr, L. Podobedova, W. L. Wiese, and K. Olsen, NIST Atomic Spectra Database (version 4), available at http://physics.nist.gov/pml/data/asd.cfm, National Institute of Standards and Technology, Gaithersburg, MD, 2009.
[25] D. R. Beck and M. H. Abdalmoneam, Bull. Am. Phys. Soc. **57**, DAMOP K1.5 (2012). Also available online at http://meetings.aps.org/Meeting/DAMOP12/Session/K1.5. A more detailed discussion can be found in "Relativistic Configuration Interaction Calculations of the Atomic Properties of Selected Transition Metal Positive Ions: Ni II, V II and W II" by M. H. Abdalmoneam, doctoral dissertation, Michigan Technological University (2015).
[26] R. D. Cowan, *The Theory of Atomic Structure and Spectra*, (Univ. California Press, Berkeley, CA, 1981) p 525.
[27] D. R. Beck, S. M. O'Malley, and L. Pan, *Computational Methods in Lanthanide and Actinide Chemistry*, (M. Dolg, editor, Wiley 2015), pps.1-21.
[28] D. R. Beck, program RPI, unpublished.
[29] D. R. Beck, program RFV, unpublished.
[30] C. W. Walter, private communication.
[31] K. T. Taylor and D. W. Norcross, Phys. Rev. A **34**, 3878 (1986).

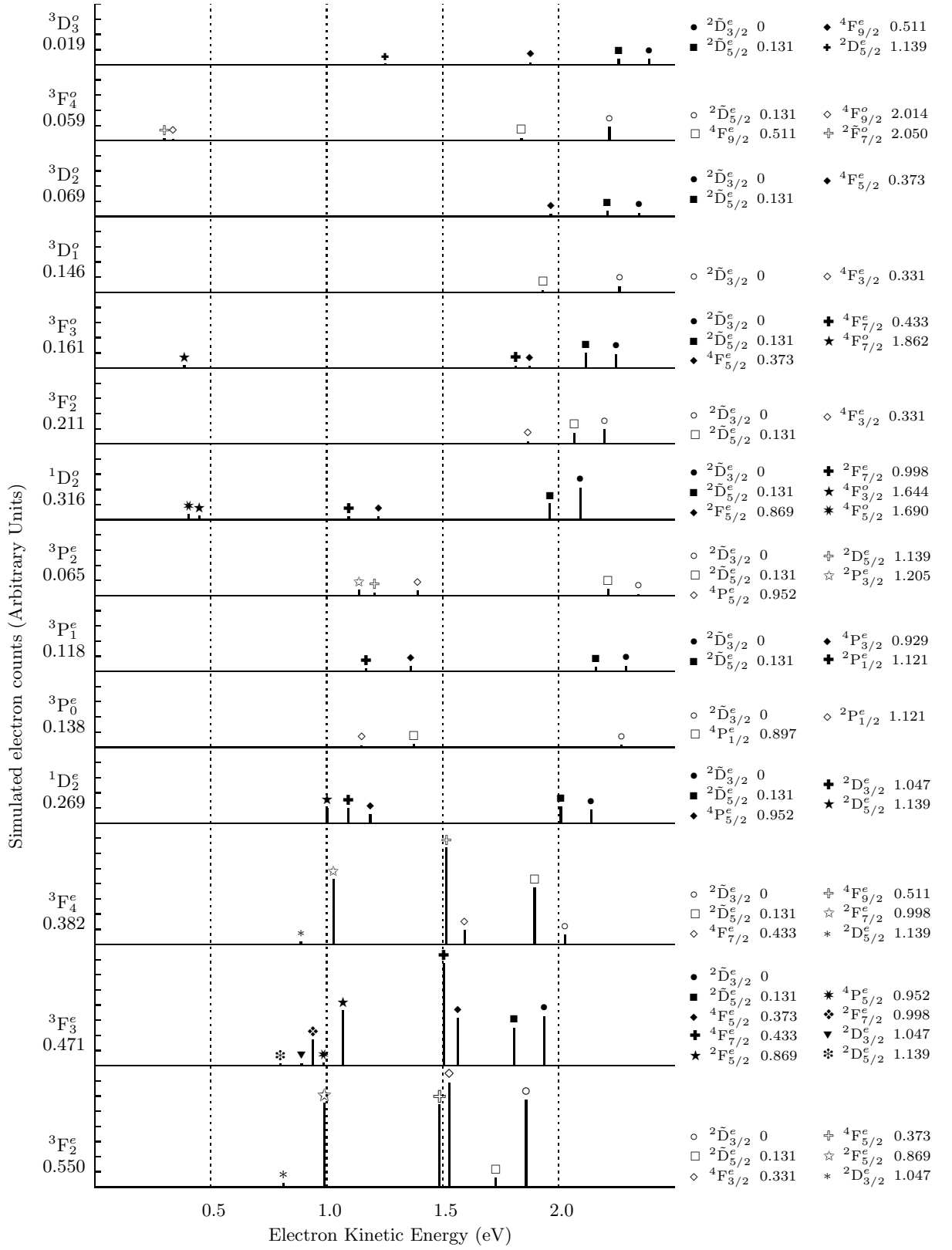

FIG. 1: Simulated electron counts using EA and BEs determined in this work, for photodetachment of La^- when the photon wavelength is 514.5 nm (2.410 eV). The effective temperature is $kT = 0.17$ eV. Starting from the bottom row are the even La^- bound states, then the odd states. The dominant LS term and binding energy (in eV) for each even ($5d^2\ 6s^2$) or odd ($5d\ 6s^2\ 6p$) La^- level are marked on the left side of the corresponding row. Each "bar" indicates the population-weighted cross section to a specific non-relativistic neutral threshold, scaled down uniformly. Only the prominent channels by the corresponding neutral threshold are included. The legend for each row lists these neutral thresholds (with energy in eV [24]), mainly $5d^2\ 6s$ ($5d\ 6s\ 6p$) for even (odd) La^- levels with the tilde in the LS term indicating $5d\ 6s^2$ ($4f\ 6s^2$) thresholds.

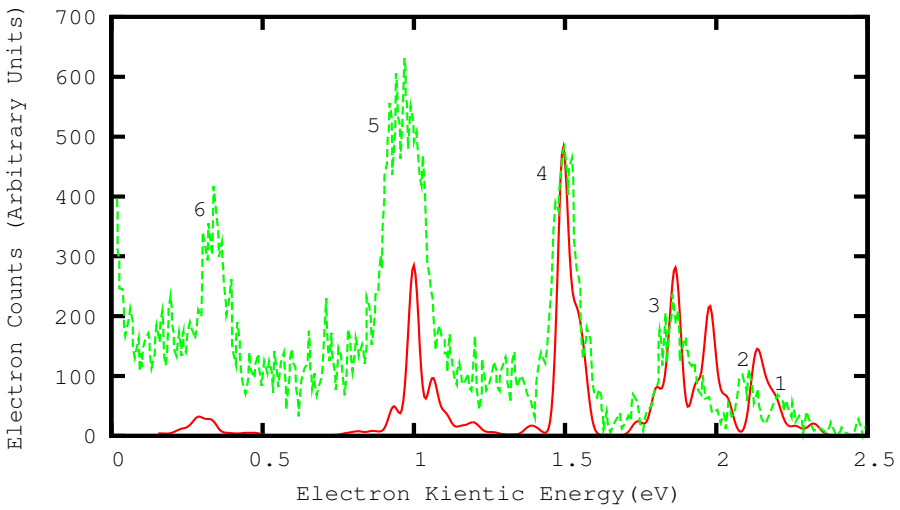

FIG. 2: Simulated electron counts plot (solid line) using early RCI binding energies by O'Malley and Beck [15]. The effective temperature is $kT = 0.17$ eV. Each channel has been convoluted with a Gaussian of full-width-at-half-maximum of 0.040 eV. The plot has been scaled so that its peak 4 has the same height as that in the experimental plot (dashed line) by Covington *et al.* [16]. The same has been done in Fig. 3 to Fig. 5. The six peaks in the experimental plot are labeled in the same way as in [16]. Note that peak 1 in the simulation lies almost halfway between peak 1 and peak 2 in the experimental plot, that peak 2 in the simulation lies between peak 2 and 3 in the experimental plot.

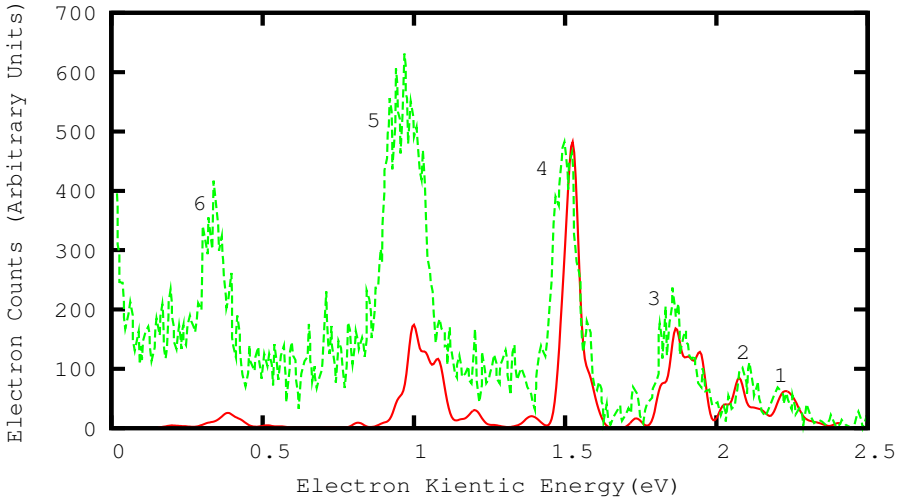

FIG. 3: Simulated electron counts plot (solid line) using La^- excited state binding energies derived from relative energies measured by Walter *et al.* [6] whenever available (details in the text), compared to the experimental plot (dashed line) by Covington *et al.* [16]. The effective temperature used in the simulation is $kT = 0.17$ eV.

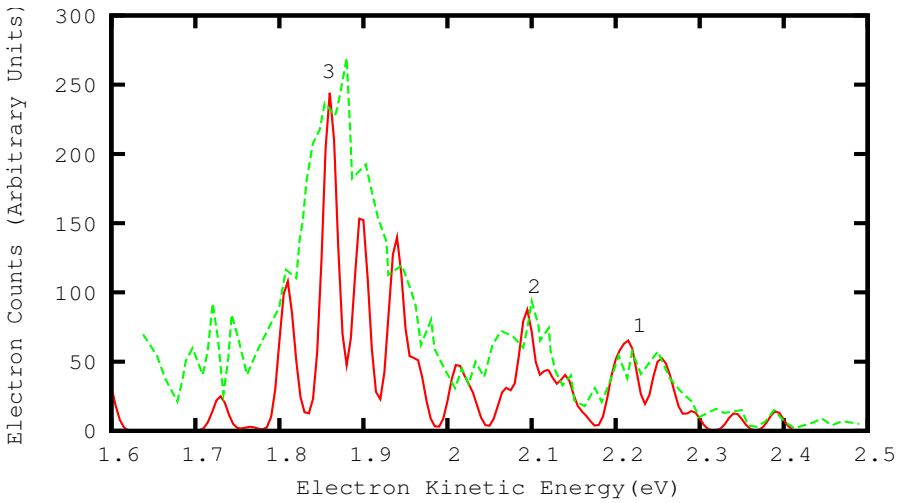

FIG. 4: The higher kinetic energy region of the simulation (solid line) at effective temperature $kT = 0.17$ eV, compared to the corresponding inset of the experimental plot (dashed line) by Covington *et al.* [16]. A smaller full-width-at-half-maximum of 0.020 eV was used in convoluting the cross sections in the simulated plot. The feature between 1.7 eV - 1.8 eV is produced by detachment of La^- ground state $^3F_2^e$ into La 5d $6s^2$ $^2D_{5/2}$.

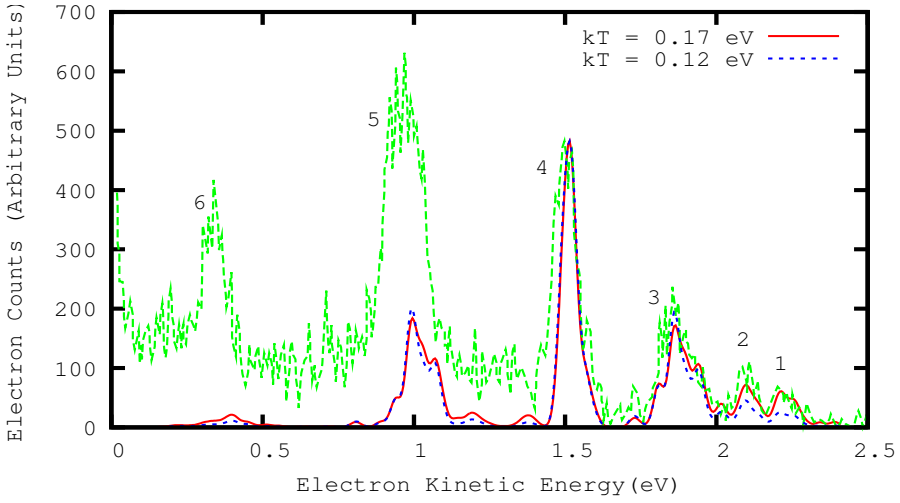

FIG. 5: Final simulated electron counts plots at two effective temperatures (kT) of 0.12 eV and 0.17 eV, compared to the experimental plot (with labelled peaks) by Covington *et al.* [16]. It can be seen changing the value of kT (from 0.17 eV to 0.12 eV) makes little difference to the overall shape of the spectrum.

TABLE I: Binding energies of La^- bound states. Units: meV

Bound State	even-parity $5d^2\ 6s^2$							odd-parity $5d\ 6s^2\ 6p$						
	$^3F_2$	$^3F_3$	$^3F_4$	$^1D_2$	$^3P_0$	$^3P_1$	$^3P_2$	$^1D_2$	$^3F_2$	$^3F_3$	$^3D_1$	$^3D_2$	$^3F_4$	$^3D_3$
Binding Energy														
RCI[a]	545	478	410	259	128	103	52	434	286	240	208	149	139	84
Experiment[b]								335.6						
This work	**550**	**471**	**382**	**269**	**138**	**118**	**65**	**316**	**211**	**161**	**146**	**69**	**59**	**19**
Relative Energy														
RCI[a]	0	67	135	286	417	442	493	111	259	305	337	396	406	461
Experiment[b]	0	83.94	172.86						343.69	383.87	399.42	470.55	496.18	538.80
Other Experiment									343.6868[c]					
											399.4757[d]			
This work	**0**	**79**	**168**	**281**	**412**	**432**	**485**	**234**	**339**	**389**	**404**	**481**	**491**	**531**
(Expt.[b] - This work)		5	5						5	-5	-5	-10	5	8

[a]Earlier RCI energy calculation by O'Malley and Beck [15]

[b]LPTS measurement by Walter *et al.* [6], with uncertainties excluded due to limited space.

[c]Measurement by Jordan *et al.* [7], with uncertainty of ±0.0015 meV.

[d]Measurement by Kellerbauer *et al.* [17], with uncertainty of ±0.0004 meV.